

## **CORROSION PERFORMANCE OF CONCRETE CYLINDER PILES**

Kingsley Lau  
University of South Florida  
4202 E. Fowler Ave. ENB118  
Tampa, FL 33620

Rodney G. Powers  
Florida Department of Transportation  
5007 NE 39<sup>th</sup> Ave.  
Gainesville, FL 32609

Alberto A. Sagüés, Ph.D.  
University of South Florida  
4202 E. Fowler Ave. ENB118  
Tampa, FL 33620

### **ABSTRACT**

Concrete cylinder piles produced by a centrifugally cast, vibrated, roller-compacted process have shown promising corrosion resistance in marine environments. Three bridges in the Florida panhandle with ~40 years in aggressive marine service and one newly constructed marine bridge utilizing concrete cylinder piles were examined. Examination of the older marine bridges showed minimal corrosion distress despite low design concrete cover over the steel hoop reinforcement (2-4 cm). Typical concrete distress included minor rust staining (not necessarily indicating corrosion of reinforcement steel) and thin longitudinal cracks (likely caused by mechanical damage from pile driving). Chloride ion diffusivity was low, in the order of  $1 \times 10^{-9}$  cm<sup>2</sup>/s. Other measured parameters such as concrete resistivity, porosity, and water absorption indicate low permeability. Chloride analysis of cracked and uncracked concrete cores from the older bridges in this study did not show pronounced preferential chloride penetration. Chloride analysis from the contemporary marine bridge did show some preferential transport of chloride ions at shallow depths through cracks with further evidence of lower electrical resistivity indicating enhanced electrolyte transport. Simplified corrosion durability modeling projections indicate that a moderate relaxation of a current 7.6 cm cover requirement may be made without significantly compromising the service life requirements of cylinder piles.

Keywords: corrosion, piles, cylinder, chloride, diffusion, durability

### **INTRODUCTION**

Post-tensioned concrete cylinder piles (often known as Raymond piles<sup>1</sup>) have been in place for many years in Florida marine bridge substructures with indications of excellent corrosion resistance. Cylinder piles typically have high cement factors, 385-474 kg/m<sup>3</sup>, and reported water to cement ratio ~ 0.35-0.45.<sup>2,3</sup> The cylinder pile segments are typically 5 m in length. During fabrication, a spiral wire cage with welded longitudinal spacing bars is placed in an assembly consisting of the cylinder pile form and end rings that maintain the placement rods that form the strand ducts typically 3.5 cm in diameter. Concrete is placed into the form that is being rotated in a process where the concrete is centrifugally cast into the form, vibrated, and roller compacted. After concrete curing and form stripping, the

segments are aligned by the duct openings for pile assembly. Long piles are made by assembling several cylinder pile segments together by post-tensioning high strength strands through the duct openings which are pressure grouted afterwards. During bridge construction, the piles are cut to length. The diameter of the cylinder piles typically range from 0.9–1.7 m. Design information for existing, older piles indicates low spiral steel clear cover ~4 cm. Cylinder piles from the Escambia Bay Bridges, inspected after ~30 years of service in aggressive marine environment in the Florida Panhandle were found to have no significant corrosion damage<sup>2</sup> despite having only ~3.5 cm average clear cover. Chloride ion diffusivity, calculated from chloride profiles of extracted concrete cores, had a median value  $<2 \times 10^{-9}$  cm<sup>2</sup>/s — among the lowest ever determined for conventional Florida bridge substructures.<sup>4</sup>

Recently implemented FDOT<sup>(1)</sup> specifications have increased clear cover to 7.6 cm and require the use of concrete pozzolanic admixtures. For the newly constructed St. George Island (SGI) Bridge in Florida, cylinder pile mix proportions reported by Gulf Coast Prestress, Inc.<sup>(2)</sup> indicate high cementitious content, ~500 kg/m<sup>3</sup> and low water to cement ratio, 0.31. However, concerns have been raised as to the feasibility and cost of fabricating cylinder piles with large clear cover without increasing risk of inducing cracks.<sup>5</sup>

In this investigation, three cylinder pile bridges with ~40 years in aggressive marine service as well as the newly constructed SGI bridge were examined (Table 1) to establish corrosion durability factors and to consider possible redefinition of cover guidelines for new cylinder pile construction.

## EXPERIMENTAL PROCEDURE

### Field Investigation Methods

All accessible marine piles (Table 1) in each of the older bridges and selected piles installed at the beginning of construction in the SGI Bridge were assessed. After visual examination, distressed areas with concrete delamination (internal separation of concrete), concrete spalls (actual, partial, or total loss of concrete cover) either pre-existing or as a result of hammer testing, and concrete cracks were noted. For piles with steel exposed during coring, half-cell potentials were measured with a copper/saturated copper sulfate reference electrode (CSE). Electrical continuity between the steel reinforcement hoop wire and strands was tested when possible to determine possible sources of corrosion macrocell phenomena.

Concrete internal relative humidity (IRH) measurements were made with a humidity/temperature probe inserted into a sealed cylindrical cavity<sup>6</sup>, bored from the pile external surface, effectively sampling the humidity of air in equilibrium with the concrete at the bottom of the cavity (3.2 cm from the exterior surface).

Concrete core samples to assess chloride penetration, 4.4 cm diameter, were extracted at the tidal and splash zones as well as at higher elevations (-0.15 to 1.5 m above high tide (AHT)). Coring was made to depths of ~8.9 cm or upon reaching post-tension strands. The cores were typically extracted in pairs along the same elevation 0.15 m apart on center and on the axis of a vertical crack if present. Additional samples include 8.9 cm diameter concrete cores from the SGI Bridge pile cutoff segments.

### Laboratory Experimental Methods

Chloride ion penetration profiles of field-extracted concrete cores were made by slice-sampling the cores, using finer slices or lathe milling near the externally exposed surface for better resolution.

---

<sup>(1)</sup> Florida Department of Transportation. 605 Suwannee St. MS30 Tallahassee, FL 32399

<sup>(2)</sup> Gulf Coast Prestress, Inc. P.O. Box 825. Pass Christian, MS 39571

The samples were analyzed for total (acid-soluble) chloride concentration<sup>7</sup>; results are given in mg of Cl<sup>-</sup> ion per gram of dry concrete. Some of the cores from unused portions of the SGI piles were ponded with salt solution following a modified Nordtest<sup>(3)</sup> method. Cut samples, ~3.8 cm in length, were sealed with epoxy leaving only the flat cut surface exposed to a 2.8 M NaCl solution for ~22 months.

Selected concrete cores were conditioned in 100% relative humidity to indirectly assess concrete permeability by monitoring concrete water absorption and electrical resistivity. Volumetric porosity was measured following ASTM<sup>(4)</sup> procedures. Internal concrete relative humidity for SGI cores was monitored initially for ambient (60-75% RH) exposure and subsequently in conditioned environments (100% RH), similar to field IRH measurements

The concrete pore water pH of selected concrete cores from the older bridges and from unused sections of SGI piles was measured using the in-situ leaching technique (ISL).<sup>8</sup>

## **CORROSION AND FORECAST DETERIORATION MODEL**

The corrosion progression of steel in concrete can be viewed as a two stage process: corrosion initiation of duration  $t_i$  (until active corrosion of reinforcing steel begins when a critical chloride threshold value is reached at the steel surface); and corrosion propagation of duration  $t_p$  (where active corrosion of steel continues until physical manifestation of concrete distress, due to the expansive corrosion products, occurs).<sup>9</sup> A durability forecast involves calculating  $t_i$  and  $t_p$  and adding them to obtain the projected service life  $t_s$ . Calculation of  $t_i$  can be made by assuming diffusional transport of chloride ions and determining the moment in which the chloride concentration  $C$  at clear cover depth  $X_c$  equals the threshold value  $C_T$  for corrosion initiation.<sup>9</sup> The piles have cylindrical geometry but because of the large pile radius to clear cover ratio a one-dimensional flat-wall geometry may be used as an approximation instead.

Assuming for simplicity Fickian diffusion with time and depth invariant diffusivity,  $D$ , and treating concrete as a homogenous medium with constant surface concentration,  $C_s$ , and uniform initial concentration,  $C_o$ , then  $C$  at depth  $x$  and time  $t$  is given by the standard solution:<sup>10</sup>

$$C(x,t) = C_s - (C_s - C_o) \operatorname{erf} \frac{x}{2\sqrt{Dt}} \quad (1)$$

The values of  $D$ ,  $C_s$ ,  $C_o$ , and  $x$  are estimated as shown later from the field observations of chloride penetration data, presence/absence of corrosion and concrete cover. The value of  $t_i$  is then obtained by inserting  $D$ ,  $C_s$ ,  $C_o$  and  $C_T$  into Eq. 1, setting  $X=X_c$  and solving for  $t$ . The value of  $t_p$  is either chosen from experience with similar systems or estimated from knowledge of corrosion rates and steel dimensions and  $X_c$ .<sup>11</sup>

The procedure indicated above can be applied also to an extended system with space-variable (by elevation) transport parameters and concrete cover. Such approach was used in a deterioration model developed for the Escambia Bay Bridges<sup>2</sup> where the region of the concrete surface where corrosion distress is most likely to occur (typically the tidal region and splash zones), is divided into small surface elements, with independent distributions of  $X_c$ ,  $D$  and  $C_s$ . Model inputs are  $C_T$ ; distributions of  $C_s$ ,  $D$ , and  $X_c$  as mean and standard deviation values abstracted from analysis of field and laboratory data or from trends identified in earlier studies<sup>2</sup>;  $t_p$ ; and the number of pile surface elements assumed to be susceptible to distress. The model output is a deterioration function given as

<sup>(3)</sup> Nordtest. Tekniikantie 12, FIN-02150 ESPOO, Finland.

<sup>(4)</sup> ASTM. 100 Bar Harbor Dr. West Conshohocken, PA 19428

the damaged fraction (number of damaged elements divided by total number of elements) of the pile surface area susceptible to damage. The model, described in detail elsewhere<sup>2</sup> was applied to the present systems where various estimates of  $C_T$  and  $t_p$  were used to calculate possible combinations of service projections. The observed corrosion-related damage from the bridge piles at the time of the survey was compared to the range of the model predictions of damage, as a tool to reveal values of  $t_p$  and  $C_T$  that best represent actual conditions.

## RESULTS AND FINDINGS

### Field Investigation<sup>(5)</sup>

**Hathaway Bridge.** The majority of 76 cylinder piles examined showed no visual signs of corrosion distress. Rust stains were observed near the pile caps of ~10% of the piles, but they are likely a result from steel exposed due to mechanical damage from pile driving. Rust stains, <200 cm<sup>2</sup>, were observed at intermediate and tidal regions on ~10% of the piles and spalled/delaminated concrete of similar size was observed on ~3% of the piles. Thin vertical cracks, 0.3 mm in width, were also observed on ~5% of piles, but no crack appeared to have been the result of expansive corrosion products.

Nearly always, steel reinforcement exposed by coring had a dull to lustrous gray mill scale appearance, with no discernable rust (Figure 1). At the bottom of one core (extracted 1.52 m AHT at a vertical crack location), the exposed spacing bar showed light corrosion in the form of faint rust-colored discoloration on part of the surface. Strand exposed by the same core showed small rust stringers with matching imprints on the surrounding grout. No cross-sectional steel loss of any significance was observed associated with these cases, and it was not clear whether the discoloration or rust represented corrosion that took place in service or prior to casting.

Half-cell potential at elevations above the tidal region, 0.3-0.9 m AHT, were always more positive than -200 mV CSE (including the light corrosion location noted above, for which potential was only -96 mV CSE) which strongly suggests that the steel at those elevations was in the passive condition at the time of inspection. More negative potentials, down to ~-700 mV CSE were measured in the lower splash zone, but no direct evidence of steel corrosion was seen there.

Concrete IRH at 1.5 m AHT was 70-75% (Table 2). IRH at 0.15 m AHT was 75-90%. The moderate IRH recorded at the atmospheric region and in one of the two measurements made at the tidal zone suggest self-desiccation of pore water indicative of concrete with a low water to cement ratio.

The cumulative distributions of spiral wire  $X_c$  values for this and the other bridges investigated are shown in Figure 4. The average  $X_c$  value for spiral reinforcement (0.64 cm diameter) for this bridge was 3.1 cm. In two cases where strand was revealed by coring, the cover was 4.4 and 5.0 cm.

**Pensacola Bay Bridge** The most common deterioration features observed were rust stains typically one per affected pile and only a few square centimeters in size, as seen on ~25% of the 908 examined piles. Larger rust stains (>100 cm<sup>2</sup>) were observed on only 15 (~2%) of the examined piles. Repair patches were frequently observed, particularly on piles in the south approach spans with ~40% of the observed rust stains on those piles associated with the patches. Concrete spalls already in place and associated with rust stains were observed only on 6 (<1%) of the examined piles; 4 of which were only of thumbnail size and very shallow. Concrete delamination, ~25–500 cm<sup>2</sup>, was revealed by hammer sounding at 9 other rust stain areas on 8 (<1%) of the examined piles. In 4 other cases, the cover concrete was found to be sound despite signs of external rust staining. Thin vertical cracks, 0.3 mm in width, were occasionally observed (~2% of examined piles) but did not appear to have been associated with steel corrosion. Hammer sounding on 2 cases with typical cracking revealed no delamination.

---

<sup>(5)</sup> A detailed description of field survey findings is given in Reference 12.

Most steel exposed by coring showed no signs of corrosion. A few instances of light corrosion of steel reinforcement and strand were observed similar to those in the Hathaway Bridge (Figure 2), all at elevations <1.2 m AHT. Appreciable corrosion loss of metal was directly observed only upon coring at two spalled/delaminated concrete areas (0.7-0.8 m AHT). That corrosion was immediately below the bottom of the spall, where as much as 25% of the wire cross section was lost (Figure 3) although only for a small length. Also, grout around strands revealed by coring in two locations appeared to have partial voids (<10 mm) suggesting partial consolidation. No evidence of corrosion was found associated with these voids, but proper casting at the steel-concrete interface is an important quality control issue for corrosion durability.

Half-cell potentials were more positive than -200 mV CSE at elevations above 1.2 m AHT, and ranged from 0 to -600 mV CSE at lower elevations. The potential for the cases of direct steel corrosion observation mentioned above was <-200 mV CSE, consistent with that expected for ongoing active corrosion.<sup>13</sup> However potentials were equally negative at several spots where direct observation showed no corrosion, and at one location 1 m AHT (not cored) where concrete was spalled the potential was only -150 mV CSE.

As shown in Table 2, IRH was 65-75% in the tidal region (0.36 m AHT) and ~60% in the atmospheric region (1.5 m AHT), suggestive of self-desiccation as noted in the Hathaway Bridge

The average concrete clear cover to hoop reinforcement was 2.33 cm, ~20% lower than in the other older cylinder pile bridges investigated. All spiral wire observed was 0.64 cm diameter. Clear cover over strand ranged from 4.7 to 6.4 cm.

**Brooks Bridge.** Little concrete corrosion-related deterioration was observed on 30 cylinder piles inspected; superficial rust staining was observed on 2 piles and shallow concrete spalling with no reinforcement exposed was observed on 2 other piles. Similar to the other bridges, thin longitudinal cracks not appearing to have been initiated by steel corrosion, 0.2 mm in width, were common. In this small sample population comprising of only 3 pile bents, the cracks were observed on ~1/3 of the piles.

Steel was exposed by coring at only 2 companion (thin crack /sound concrete) locations 0.15 m AHT; steel (spiral wire) exposed at the crack core showed no direct evidence of corrosion. Light corrosion was observed as discoloration on part of the spiral wire and spacing bar exposed at the sound concrete companion core.

Potentials were more positive than -200 mV CSE above 0.6 m AHT. Potentials as low as -700 mV CSE were measured in the tidal/lower-splash regions. Potential at the location of the cores mentioned above was ~-400 mV CSE.

The average concrete clear cover to hoop reinforcement there was 2.9 cm. All spiral wire was 0.64 cm diameter. Strand was not exposed in any of the corings of this bridge.

**St. George Island Bridge.** The SGI Bridge reflects current design specifications used in Florida including thicker design clear cover for spiral reinforcement. Also, the concrete mixture proportions included ~22% fly ash cement replacement and 8% microsilica cement replacements for segments above tide level. A limited inspection of fifteen piles was conducted, twelve of which were being evaluated for a construction-related assessment independent of the present investigation. Those twelve piles had superficial rust staining or fine longitudinal cracks that are not likely related to corrosion of reinforcement steel<sup>(6)</sup>. Two of the remaining three piles, among those earliest erected during construction had thin longitudinal cracks 0.051 mm in width. No cases of corrosion of spiral reinforcement were found. Half-cell potentials more positive than -200 mV CSE were observed at pile

---

<sup>(6)</sup> A separate investigation of construction issues on those piles, unrelated to this work is in progress and will not be addressed here.

elevations above 0.6 m AHT. As in the other bridges, more negative potentials were measured at lower elevations (as low as -600 mV CSE). The spiral reinforcement (0.95 cm diameter) clear cover was 7.2-8.9 cm, consistent with design specifications. Strand was not exposed during coring.

## Laboratory Experiment Findings

**Chloride Ion Penetration Profiles Observations and Diffusion Parameters.** Figures 5 and 6 show examples of chloride penetration profiles from field extracted cores on sound and cracked concrete. Idealized chloride penetration profiles were calculated for sound concrete data using least square error fitting (per Eq.1) of the data, yielding values of the apparent diffusivity,  $D_{app}$ , and  $C_s$  as well as  $C_o$  (which was normally quite small and neglected in the following). Figures 7 and 8 show cumulative distributions of the  $D_{app}$  and  $C_s$  obtained for each of the structures assessed as well as for the previously examined Escambia Bay Bridges. Notably values of  $D_{app}$  are very low. The overall median  $D_{app}$  was only  $\sim 1e-9$   $cm^2/s$ , which is less than the median value recently obtained for modern conventional concrete structures in Florida built for aggressive marine service,  $\sim 4e-9$   $cm^2/s$ . The range of diffusivity values observed is also comparable to those obtained for the Escambia Bay Bridges, underscoring the overall low permeability of the concrete in cylinder piles.

The  $D_{app}$  values obtained for the Brooks Bridge samples are on the average 3 times greater than for the other three bridges of similar age, but it should be noted that only 4 samples were evaluated and all came from a single pile. Consequently, without additional samples from other locations in that bridge it cannot be ascertained whether the concrete used in those piles was more permeable than in the comparable bridges. Of more varied origins were the data for the new SGI Bridge, which include cores from two piles in service, to which have been added data from laboratory ponding tests of cores extracted from unused pile sections. Chloride penetration was shallow as expected for the limited time of service in seawater. Nevertheless, the overall results tended to show values comparable to those obtained in the other, much older structures. It is recalled that concrete with pozzolanic additions tends to show a markedly decreasing  $D_{app}$  trend with time reflecting decreasing connectivity of the pore network as the pozzolanic reactions progress.<sup>14</sup> Thus, it is expected that concrete in the SGI Bridge will show lower  $D_{app}$  values in the future.

In agreement with a commonly observed trend in marine substructure,  $D_{app}$  and  $C_s$  tended to decrease with increasing elevation as shown in the composite graphs in figures 9 and 10 (including the Escambia Bay Bridges data). The trend is expected as the water content of the concrete decreases with increasing elevation, with consequent reduction in the ion transport ability through the concrete.

The typical chloride ion concentration of the water traversed by the bridges is listed in Table 1. Figure 11 shows that the ranges of  $C_s$  values observed in the various bridges investigated are roughly independent of the chloride content of water in the span of salinity encountered. The similarly overlapping data from an additional sampling of Florida bridge substructures<sup>4</sup> made with conventional concrete is also shown. This behavior reflects the development of nearly salt-saturation conditions (and hence approximately equal concentration independent of salinity of the source) on much of the surface of the concrete by evaporative concentration of marine water.<sup>15</sup>

When exposed by coring, the longitudinal cracks noted earlier were often found to run the entire length of the core. It is of much interest to determine whether preferential chloride ingress along the cracks (and consequent localized corrosion initiation) could become important. Examination of the chloride profiles obtained in this investigation (exemplified by those in figures 5 and 6) showed no indication or only limited indication of enhanced chloride penetration through cracks. The cases showing some preferential penetration were usually much less developed than the dramatic examples of enhanced chloride penetration documented elsewhere for some conventional concrete FDOT marine substructure.<sup>4</sup> In addition, the present steel corrosion survey failed to show any clear association between prior presence of cracks and preferential corrosion initiation, even in the bridges that had been in service for 40 years. Consequently, there is no clear indication at present that fast chloride transport

at thin cracks is a significant corrosion initiation factor in cylinder piles, at least for those built with relatively low external clear concrete cover.

**Concrete Permeation Properties.** Near-terminal wet resistivity values (~100 days of humidity exposure) listed in Table 2, were usually high, in the order of 100 kΩ-cm for the older bridges<sup>(7)</sup>. Resistivity values from the SGI Bridge cutoff sections were even higher, consistent with the expected high concrete quality with pozzolanic additions. Limestone aggregate cores tended to have the highest wet resistivity values observed. Notably, the resistivity of the SGI Bridge cores (primarily limestone) in service drilled on cracks was noticeably smaller than that of the peer cores on sound concrete. This behavior suggests enhanced ionic transport through the crack region, consistent with indications of some (but not necessarily dramatic) preferential chloride penetration at cracks noted earlier.

Volumetric porosity measurements made for concrete core fragments extracted from the bridges are shown in Table 2. Low porosity for the ~40 year old bridges was consistent with the expected low water to cement ratio and the advanced hydration age of the concrete. Volumetric porosity measurements from two SGI Bridge cutoff concrete mixes (limestone) had similar results (~8-11%); the other concrete mix (river rock) showed higher porosity (~13%) consistent with observation of lower wet resistivity as well.

Initially when the SGI Bridge cores were stored in ambient laboratory conditions, the IRH reflected a similar range to its environment (60-75% RH). The moisture pickup in the core samples exposed to conditioning in a 100% RH chamber, as measured by IRH only began to show signs of stabilization after ~100-200 days which may be indication of low permeability. Moisture pickup (95% RH) in the laboratory samples would be higher than actual field conditions due to the increase in exposed surface area.

**Concrete Pore Water pH.** For SGI Bridge cutoff samples, 12 pH measurements were made from 6 cores. Terminal pH values, 12.8 to 13.5, were within the commonly observed range for present day concretes<sup>8</sup>, so it appears that the pozzolanic additions did not result in a pronounced drop in pore water pH. A total of 17 pH measurements were made from 8 concrete core samples from the older bridges. One measurement had a terminal pH value ~13, and in another as low as ~11. The 15 other measurements yielded values between 12 and 13. Experimental artifacts, likely when using small cored specimens of highly impermeable concrete, may account for some of the lowest values observed. The overall modest pH values observed in the older bridge samples are nevertheless intriguing, considering that these older piles were expected to be made using unblended cement, and that pH lowering processes such as carbonation do not penetrate deeply in lower marine substructure elements.<sup>6</sup> It is possible however that the cements used in the older piles had lower alkali content than modern cements.

## DISCUSSION

### Pile Field Performance

Findings are indicative of very good corrosion resistance of older cylinder piles over service periods of several decades, consistent with earlier findings for the Escambia Bay Bridges. Exceptions were locations such as the upper end of the pile by the pile cap, where mechanical distress during construction had exposed reinforcement that was not sufficiently protected afterwards. Conspicuous rust stains at intermediate elevations appear in most cases to have resulted from corroding steel debris or other auxiliary components but not related to corroding reinforcement or strand.

---

<sup>(7)</sup> Although all values were corrected for specimen dimensions, some short specimens from the Pensacola Bay Bridge may have been subject to test artifacts as they yielded resistivity values that were still high, but ~2/3 lower than those of normal size specimens.

No telltale rust patterns on the surface of the piles, reflecting the position of spiral reinforcement or strand, were noticed upon examination. Extraction of cores focused on spots selected for showing unusually high rust staining, and yet only two cases of appreciable loss of steel due to corrosion were found in the three older bridges investigated. All of the other observations of steel corrosion (including some on the post-tensioning strand) were of only minor rust or discoloration, some of which may have been present prior to embedment in concrete or grout. Steel potentials were generally noble (indicative of a passive condition at the time of the measurements) over much of the elevation range above the lower splash zone ( $\sim >0.6$  m AHT).<sup>(8)</sup> The general evidence of little or no corrosion of the older bridges is striking in view of the aggressiveness of the environment, the four-decade long service life of the structures investigated, and the thin clear cover existing.

The observed high corrosion resistance of the older piles appears to stem from a combination of very low chloride penetration rates with either or both of the following: a substantial value of  $C_T$ , and low corrosion propagation rates if  $C_T$  was exceeded. These factors are considered next.

## Chloride Penetration

The range of surface chloride concentrations observed were similar to those encountered in other marine and estuarial Florida bridges built with conventional concrete (Figure 11). Thus the driving force for chloride penetration in the cylinder piles was not unusually high or low. The observed chloride diffusivities were however extremely small (median  $10^{-9}$  cm<sup>2</sup>/s) which indicate chloride penetration to be greatly retarded in the bulk of the concrete. Furthermore, in contrast to observations in conventional Florida marine substructures, rapid chloride transport through thin cracks was not strongly apparent in the older cylinder piles (Figure 5). Thus, even though thin cracks were frequently observed, inward chloride ion penetration appeared to be mainly a function of bulk parameters.

Low bulk chloride diffusivity was expected in high quality concrete with high cement content, low water to cement ratio and good compaction, as used in the cylinder piles. Both the low bulk diffusivity and the lesser importance of thin cracks may have been promoted by moderate internal concrete moisture as indicated by the low internal RH levels often measured in the field. Low internal moisture can exist even under wet external conditions if the concrete is dense and the low water to cement ratio induces self-desiccation upon long term hydration of the cement.<sup>17</sup> Under those conditions ionic transport in the bulk, already slow due to a tight pore network, is made slower by fewer liquid paths within the pores. Transport in thin cracks is lowered as well, since the presence of liquid along the crack line is equally diminished. This condition is manifested, for example, by the lesser importance of crack transport even in conventional substructure, when cores containing cracks are extracted at higher elevations where the concrete is drier<sup>4</sup>.

The above considerations apply also to the newly formulated piles at the SGI Bridge but attention is called to the somewhat higher (but still quite small in absolute terms,  $3e-9$  cm<sup>2</sup>/s) diffusivity encountered in one of those piles. Nevertheless, because of the high pozzolanic content of the SGI Bridge concrete, bulk chloride transport is expected to become even slower in the future. The thin cracks in the SGI Bridge piles in some instances propagated deep into the reinforcement level, and limited preferential chloride ingress was observed in the shallow range ( $\sim 1$  cm) where chloride profiles were measurable (Figure 5). It is possible however that the same conditions that seem responsible for mitigating chloride crack transport in the older bridge piles will be active here as well.

It is noted that in all cases longitudinal steel strands are placed about 1/3 to 1/2 deeper than the spiral wires or spacing bars so, all else being equal, the value of  $t_i$  for the strands is expected to be considerably longer than for the other steel components considered here.

---

<sup>(8)</sup> It is noted that while noble potentials are usually associated with a passive steel condition, more negative potentials are not necessarily indicative of active corrosion in progress<sup>21</sup>.



## Critical Chloride Threshold

Because most corrosion observations involved cases where there was only minor rust discoloration, it is uncertain in those instances whether sustained active corrosion was actually in progress. Indeed, in some instances with light corrosion, the steel potential readings were indicative of passive conditions. A mainly conservative chloride threshold estimate can be made nevertheless by assuming that these cases represent active corrosion in progress, and calculating the value of the chloride concentration at the corresponding steel depth. To that end, the data on the condition of the spiral wire and spacing bar reinforcement and chloride concentration at the recorded steel depth were used to construct the composite cumulative distribution graph for the older bridges shown in Figure 12. The chloride concentration at the time of the survey (although for the two severe corrosion instances corrosion initiation probably took place much earlier) at the steel depth was calculated from the diffusion parameters determined by analysis of the core that exposed the steel. If no chloride or accurate cover data were available for a core, estimates were made from nearby core data.

The trend in Figure 12 (although affected by large uncertainty from the many assumptions made) suggests that no corrosion initiation took place at concentrations  $<0.5$  mg/g ( $1.2$  kg/m<sup>3</sup>), but that in many instances the chloride content was higher and not even incipient signs that corrosion had taken place were observed. Thus a value of  $0.5$  mg/g may be suggested as a conservative lower bound for the critical chloride threshold of reinforcing steel in these piles, recognizing that the actual effective threshold value or range of values is likely to be significantly greater due to the stochastic nature of corrosion initiation. It is worthwhile noting that  $C_T$  values reported in the literature for steel in conventional concrete but with high cement content similar to that present in cylinder piles are in the order of  $\sim 1$  mg/g ( $2.4$  kg/m<sup>3</sup>).<sup>18</sup> Factors such as better concrete compaction in the cylinder piles may result in higher threshold values compared with that in conventional cast concrete. In any event, given the  $C_T$  values suggested by this analysis and the  $X_c$ ,  $C_s$  and  $D_{app}$  ranges obtained, it appears that at the time of the survey corrosion initiation was just beginning to affect a small fraction of the pile inventory of the older bridges.

Chloride threshold cannot be directly evaluated for the SGI Bridge as no reinforcement corrosion cases were documented (rust spots seen on the surface of some SGI Bridge piles appear to be related to steel debris or other extraneous sources). However, the pore water assessment indicated a high pH in spite of the high pozzolanic content. Thus, it appears likely that normal chloride threshold values may apply.

The above discussion applies to spiral or rebar steel. Little can be said from the present findings about the effective threshold for the strand as penetration to strand depth was very small, and the few instances of rust on strand were not clearly related to ongoing corrosion. In the absence of other information, it will be assumed that the corrosion threshold for properly grouted strand is comparable to that of the other steel in these structures, with consequent expectation of much longer times to corrosion initiation due to the deeper clear cover of the strand. The presence of grout voids around the strand, as observed in two cases in the Pensacola Bay Bridge, may locally lower the corrosion threshold. Control of grouting quality is essential.

## Corrosion Propagation Rates

From general observations of low external manifestations of corrosion, it can be said that corrosion propagation (topical extraneous damage excluded) had either not commenced in most of the piles, or was proceeding at a very low rate. With the exception of two severe corrosion cases in the Pensacola Bay Bridge, the steel exposed by coring that showed some signs of corrosion had very small average corrosion penetration, perhaps only a few micrometers. If that corrosion actually occurred in service, the previous discussion suggests that initiation took place relatively recently, so typical corrosion propagation rates may be in the micrometer per year range (barely above usual estimates of passive corrosion rates).<sup>(19)</sup> This modest range estimate is not surprising considering that the concrete

in the piles, even when wet, had high resistivity (reflecting low pore connectivity and often moderate internal humidity), of a level commonly associated with very low or negligible corrosion rates. In the wetter parts of the substructure oxygen diffusivity would be expected to be low, further lowering the overall corrosion rate.

The time necessary for a corrosion-induced crack to occur may be evaluated using the expression by Torres-Acosta<sup>11</sup>,

$$X_{\text{CRIT}} \text{ (mm)} \sim 0.011 \left( \frac{X_c}{\Phi} \right) \left( \frac{X_c}{L} + 1 \right)^2 \quad (2)$$

where  $X_{\text{CRIT}}$  is the steel corrosion penetration necessary to cause a crack in the concrete,  $X_c$  is the concrete cover thickness,  $\Phi$  is the steel bar diameter, and  $L$  is the corroding length. Assuming conservatively that  $L \gg X_c$  and taking representative dimensions for the spiral wire in the older bridges ( $\Phi=6\text{mm}$  and  $X_c=30\text{mm}$ ) the result is  $X_{\text{CRIT}} \sim 0.05 \text{ mm}$ . However if  $L \sim X_c$ , as in early initiation events,  $X_{\text{CRIT}}$  would be twice as large. With corrosion rates in the order of those estimated above the typical time required to develop a corrosion induced crack after the initiation event could easily stretch into tens of years.

After the first corrosion induced cracks take place the corrosion rate is likely to increase so subsequent deterioration would be faster and concrete delamination would quickly ensue. The two recorded incidents of severe wire corrosion may reflect such occurrence. In one of those cases the estimated clear cover was only 1.4 cm, and corrosion propagation may have been in progress for many years already. It is noted that even in those cases, the actual metal loss was quite localized and much of each wire segment extracted retained the initial dimensions.

### Forecast Model Analysis

Forecast model input values based on the above discussion are listed in Table 3. The model output is reported as the deteriorated fraction of the susceptible pile surface of a generic case representative of the three older bridges. The average calculated  $D_{\text{app}}$  of the concrete from the Hathaway and Pensacola Bay bridges was used as the mean value for that parameter. A standard deviation value  $\sigma$  for chloride ion diffusivity of one-half of the mean value was assumed by analogy with observations in the Escambia Bay Bridges investigation.<sup>2</sup>

Although no continuous distributions were used for  $C_T$  and  $t_p$ , the calculations included damage projections with alternative combinations of those parameters. Two  $C_T$  values were chosen: a low value equal to the lower bound estimated earlier, 0.5 mg/g (1.2 kg/m<sup>3</sup>), and a high value equal to the highest chloride content measured (5.8 mg/g (13.5 kg/m<sup>3</sup>)) for a field sample that had no corrosion distress of the reinforcing steel. High chloride threshold values may be possible considering that the concrete has a high cement factor, and in the cases of the older bridges, an absence of pozzolanic materials.<sup>20</sup> Polarization effects can also substantially increase  $C_T$  as still passive portions of the steel reinforcement may be cathodically prevented from corrosion initiation by galvanic coupling with an active corrosion site;  $C_T$  values as large as 17 kg/m<sup>3</sup> have been reported for laboratory concrete samples under those circumstance.<sup>21</sup> The values of  $t_p$  chosen were 12, 24 and 48 years (assumed as fixed values<sup>2</sup>). Such large  $t_p$  values, as suggested by the earlier discussion, may stem from limited transport of oxygen to the steel surface, high concrete resistivity or small reinforcing wire diameter.

Figure 13 shows the resulting deterioration forecast model outputs to which are superimposed bounded ranges of values representing the actual damage in each bridge at the time of the survey. The actual damage was bounded by a conservative upper limit where each observed rust spot is

considered to represent one distressed element (although as indicated earlier many rust spots were not related to reinforcement damage). The lower bound limit is the amount of corrosion-induced damage confirmed by direct observations (not related to mechanical damage or other preexisting circumstances) in the bridge. In the case of the Brooks Bridge no damage fell in that category, so a lower limit was assigned as corresponding to at least one distressed element that may have escaped detection during the survey.

In Figure 13 the projections resulting from the various  $t_p$ - $C_T$  combinations are labeled A through F. Combination A (lowest  $t_p$  and  $C_T$  values) greatly over-projects the damage at the time of survey and is too conservative. Combination F (high extremes of  $t_p$  and  $C_T$ ) is clearly too optimistic. Thus the actual damage range was better represented by the combinations of intermediate discrete  $t_p$  and  $C_T$  values. Because of the cathodic prevention effects mentioned earlier<sup>21</sup>, lower  $C_T$  values are expected to be prevalent earlier in the life of the bridges, while higher values may exist near the end. Thus, combinations B-C (or even A) may better describe earlier behavior while D-F may apply to the later stages. If low  $C_T$  values dominate earlier behavior, then propagation times that are short or very short (e.g. 5 years, as often assumed for other marine substructure or deicing salt service cases<sup>4</sup>) do not seem likely as the resulting projected damage would greatly over-predict observations. This outcome is consistent with the expectation, from the previous discussion, that the corrosion durability of concrete cylinder piles benefited from long propagation times ( $>12$  years assuming  $1.2 \text{ kg/m}^3 < C_T < 13.5 \text{ kg/m}^3$ ).

The service life of a pile substructure can be nominally defined as the time when a given fraction of the pile surface elements is projected to be distressed. As a working example, Fig. 10 includes horizontal lines for 1% to 10% damage representing the development of ~ 4 to 40 damaged elements (combined area ~0.06 to 0.6  $\text{m}^2$ , respectively, which is in the order of the size of a typical repair patch<sup>2</sup>) on each pile of the bridge. Such level of distress may not represent severe structural damage but could require extensive maintenance repairs with considerable cost. The nominal service life range corresponding to the 1%-10% damage level depends on the parameter combinations assumed. If as suggested above actual performance falls somewhere between the B-C and D-E scenarios, the model then projects that nominal service life for the older bridges may extend some decades into the future. Such projection is also consistent with the generally good present condition, and generally agrees with the earlier analysis of the Escambia Bay bridges.<sup>2</sup> The results suggest that these older cylinder pile bridges have performance prognoses that rival or exceed those sought under present day 75-year design service life goals.

### Issues on Clear Cover Specification

The model calculations can be used also to examine the consequences of relaxing the present clear cover specification ( $X_c=7.6$  cm) to lower values to address possible fabrication and economic concerns as indicated in the Introduction. As shown earlier, the range of  $D_{app}$  and  $C_s$  values for the SGI Bridge, representative of new construction, was similar to that of the older bridges, and  $C_T$  is not expected to be very different either. Thus, the input model parameters used for Figure 13 can be left the same and mean  $X_c$  varied from the base value of 2.96 cm while keeping variability and truncation at realistic values (Table 3). This has been done and case B is used as an example, since per the previous discussion actual performance is better represented by the intermediate scenarios. The model outputs are shown in Figure 13 by dashed lines. Case Bp is for the present design value  $X_c=7.6$  cm, and case Ba addresses a relaxed cover alternative  $X_c=5.1$  cm representing a possible compromise of cost, fabrication feasibility and durability. Case Bp shows dramatic projected performance improvement over B, which could be expected since per Eq. 1  $t_i$  increases with the square of  $X_c$  and in Case B the initiation period is an important contribution to the overall time to corrosion (see next paragraph). For the same reason, case Ba shows lesser but still substantial improvement. Similar analysis with the other cases showed comparable results. These estimates suggest that, from a bulk chloride penetration standpoint, cylinder piles constructed with the materials examined here could have clear cover levels moderately lower than the currently specified value and still be consistent with a 75 year durability goal.

The model calculations do not consider the potential for localized chloride ingress paths; notably preexisting cracks may be of concern. Thus in addition to lower lowered material requirements and fewer fabrication constraints, a smaller cover might also reduce the propensity for incidence of cracks, especially if admixtures such as microsilica create less tolerance to curing anomalies.<sup>16</sup> Improved reliability may result as well as fabrication methods would approach established practice that has resulted in the good corrosion performance documented here for the older piles. It is noted nevertheless that considerations of clear cover relaxation should be made in the context of the other structural and economical issues determining performance of concrete cylinder piles. Of special interest is the condition of the strand at the joints between the pile segments where epoxy or similar filler materials are placed as a seal. A reduction in design cover would also reduce the length of the thin polymer-filled region between the segment faces possibly facilitating chloride ingress at the joint. Special provisions for added quality control or supplemental protection there should be considered. It is noted however that no particular association between pile joints and evidence of corrosion was noted in the survey of the older bridges.

## CONCLUSIONS

1. Examination of three 40 year old cylinder pile bridges (Hathaway, Pensacola Bay, and Brooks) indicated in general that only minor or no corrosion distress of the spiral reinforcement or strand in the piles had taken place in spite of small clear concrete cover values of 10 to 39 mm. Some corrosion noted near pile caps or the presence of topical patches, appear to reflect early mechanical damage unrelated to normal exposure. Similar good corrosion performance was found in a previous examination of the Escambia Bay bridges, also built with cylinder piles.
2. The rate of chloride ion penetration in the 40-year old bridges, as indicated by the apparent diffusion coefficient, had a median value of only  $\sim 1 \times 10^{-9}$  cm<sup>2</sup>/s, lower than that of modern concretes specified for aggressive marine service. High electrical resistivity and moderate internal humidity of the concrete were consistent with the slow chloride transport observed. These properties appear to have resulted from high cement content, low water to cement ratio, and good compaction inherent to the pile fabrication process.
3. Thin (<0.3 mm) concrete cracks were observed in some of the piles in the 40-year old bridges. However, unlike behavior recently noted in other bridges with conventional concrete substructure, preferential chloride penetration along the crack was less pronounced.
4. Tests of the early performance (~2 years) of new cylinder piles built to current guidelines (thicker cover, pozzolanic admixtures) also show excellent average resistance to chloride penetration. Thin cracks were observed here as well, together with evidence of enhanced chloride penetration at shallow depths.
5. The survey information from the older bridges was used to estimate a lower bound value for the chloride threshold for corrosion initiation in the order of 1.2 kg/m<sup>3</sup>. This bound is consistent with the reported high cement content of the concrete and the observation of pH values in extracted cores approaching normally expected values. Effective threshold values could be significantly higher. The concrete in the new bridge piles had a desirably high pore water pH despite its high pozzolanic content, suggesting that chloride threshold values in the new material will be in the normal range.
6. Simplified corrosion damage forecasts for the older and new piles suggest that very long service lives with minimum corrosion-related maintenance are possible. Moderate relaxation of absolute minimum cover requirements for new construction may be feasible without severely compromising the corrosion durability of cylinder piles.

## ACKNOWLEDGMENT

The support of the University of South Florida Corrosion Engineering Laboratory and the Florida Department of Transportation Corrosion Laboratory is gratefully acknowledged. The opinions, findings and conclusions expressed in this publication are those of the authors and not necessarily those of the State of Florida Department of Transportation or the U.S. Department of Transportation.

## REFERENCES

1. Scannel, W., F. Soh, A. Sohangpurwala, and A. Sagüés. "Assessment of Rehabilitation Alternatives for Bridge Substructure Components." Final Report, CONCORR, Inc. Ashburn, Virginia, 1997.
2. Sagüés, A.A., Corrosion. Vol.59, no.10. p.854-866, 2003.
3. LeMieux, G.F., Concrete International. Vol. 20, no.2. p.67-70, 1998.
4. Sagüés, A.A. and S.C. Kranc. "Corrosion Forecasting for 75-Year Durability Design of Reinforced Concrete." Final Report to Florida D.O.T. WPI 0510805, Contract No. BA-502. December, 2001. Available online, [www.dot.state.fl.us](http://www.dot.state.fl.us).
5. Avent, R.R. and D.J. Mukal. "Investigation of Cracks in Cylindrical Spun-Cast Concrete Piles in a Marine Environment." Final Report for Louisiana Transportation Research Center. 1998.
6. Sagüés, A.A., et al. "Carbonation in Concrete and Effect on Steel Corrosion." Final Report to Florida D.O.T. WPI. No. 0510685. June 1997. Available [www.ntis.gov/search](http://www.ntis.gov/search).
7. Florida Method of Test for Determining Low-Levels of Chloride in Concrete and Raw Materials. FM-5-516 (2000).
8. Sagues, A.A., S.C. Kranc, L. Caseres et al. "In-core Leaching of Chloride for Prediction of Corrosion of Steel in Concrete". Long Term Durability of Structural Materials. P.J.M. Monteiro, K.P. Chong, J. Larsen-Basse, K. Konvopoulos. Elsevier Science, Ltd. 2001.
9. Tuuti, K. "Corrosion of Steel in Concrete." Swedish Cement and Concrete Research Inst, 1982.
10. Crank, J. The Mathematics of Diffusion. 2<sup>nd</sup> edition. Oxford: Clarendon Press, 1975.
11. Torres-Acosta, A.A. and A.A. Sagüés. ACI Materials Journal. Vol. 101, no.6. p.501-507, 2004.
12. Lau, K., A.A. Sagüés, and L. Yao. "Corrosion Performance of Concrete Cylinder Piles." Final Report to Florida D.O.T. Contract No. BC353 RPWO#10. February 28, 2005.
13. Half-Cell Potentials of Uncoated Reinforcing Steel in Concrete. ASTM C876. (1991).
14. Bamforth, P. "Improving the Durability of Concrete by the Use of Mineral Additives." Paper presented at Concrete Durability in the Arabian Gulf, Bahrain Society of Engineers, March 1995.
15. Sagüés, A.A. et al. "Corrosion Resistance and Service Life of Drainage Culverts." Final Report to Florida D.O.T., WPI NO. 0510756. August 2001. Available online, [www.dot.state.fl.us](http://www.dot.state.fl.us).
16. Diamond, Sidney, S. Sahu and N. Thaulow. Cement and Concrete Research. Vol.34, p.1625-32, 2004.

17. Nilsson, L.O., "Moisture in Marine Concrete Structures." In Durability of Concrete in Saline Environment. Lund: Cementa AB, 1996.
18. Li, Lianfang. Corrosion. Vol. 57, no. 1, p.19-28, 2001.
19. Sagüés A.A., M.A. Pech-Canul and Shahid Al-Mansur. Corrosion Science, Vol.45, p.7. 2003.
20. Bentur, A, S. Diamond and N.S. Berke. Steel Corrosion in Concrete. London: E&FN Spon, 1997.
21. Presuel-Moreno, F.J., A.A. Sagüés, and S.C. Kranc. Corrosion. Vol. 61, no. 5, p. 428-436, 2005.

**TABLE 1  
SURVEYED BRIDGES**

Bridge	Number	Year Built	Inspection Date	Location	Water Cl <sup>-</sup> Content (ppm) <sup>†</sup>	Length	Examined Piles / Total Piles	Pile Diameter
Hathaway	460012	1960	Dec. 2002	Panama City, FL	25 560	1 024 m	76 /76	1.37 m
Pensacola Bay	480035	1960	March 2003	Pensacola, FL	7 374	4 767 m	908 /916	1.37 m
Brooks	570034	1964	March 2003	Ft. Walton Beach, FL	9 833	402 m	30 /80	0.91 m
St. George Island	490003	2003	March 2004	St. George Island, FL	8 875	6 588 m	15 /~646	1.37 m

† FDOT records.

**TABLE 2  
CONCRETE PERMEATION PROPERTIES**

Bridge	Aggregate Type	Median Diffusivity (cm <sup>2</sup> /s)	Wet Resistivity (kΩ-cm)	Porosity (%)	IRH (%)
Hathaway	River Rock	4.4e-10	100-200	6-7	70-75 <sup>†</sup> 75-90 <sup>‡</sup>
Pensacola Bay	River Rock	7.8e-10	70-100 25-50	9	65-75 <sup>†</sup> 60 <sup>‡</sup>
SGI in-service	Limestone		50-100 crack 70-200 sound	-	-
	878 River Rock	1.4e-9	100	13	-
943 and 1404	Limestone		200	8-11	60-75 <sup>*</sup> 95 <sup>**</sup>

† Atmospheric exposure region 1.5 m AHT. ‡ Tidal region 0.15-0.36 m AHT. \* Ambient dry condition 60-75%RH (lab specimen geometry). \*\* After ~100-200 days in 100% RH environment (lab specimen geometry).

**TABLE 3  
FORECAST MODEL INPUTS**

	Older Bridges Case	SGI Bridge Cases	
Surface element (m <sup>2</sup> )	0.016	0.016	
Elevation range (m)	1.5		
Mean chloride ion diffusivity D	1.18e-13 <sup>†</sup>	1.18e-13 <sup>†</sup>	
Standard deviation $\sigma$	9.84e-14 <sup>‡</sup>	9.84e-14 <sup>‡</sup>	
Min. D truncation (m <sup>2</sup> /s)	0	0	
Mean Cl <sup>-</sup> surface concentration Cs	20	20	
Standard deviation $\sigma$	6.0	6.0	
Min. Cs truncation	0	0	
Max. Cs truncation (kg/m <sup>3</sup> )	40	40	
Mean clear cover Xc	2.96	8.1	5.1 <sup>*</sup>
Standard deviation $\sigma$	0.43	0.43	0.43
Min. Xc truncation (cm)	1.0	7.2	5.0 <sup>*</sup>

† Avg. value from Hathaway and Pensacola Bay bridges. ‡  $\sigma \sim 0.5$  mean.<sup>1</sup> \*Example Xc reduction.



**FIGURE 1- Exposed spiral wire, no corrosion. Pile H29-3.**

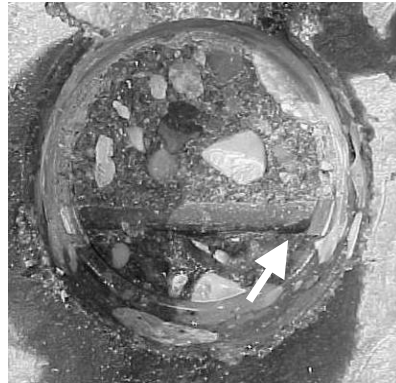


**FIGURE 2- Exposed spiral wire, light corrosion. Pile P110-2. Arrow indicates minor rust discoloration.**



**FIGURE 3- Extracted spiral wire, severe corrosion. Spiral wire from P149-2, 0.64 cm diameter, showing appreciable localized loss of cross section at the right end of the segment cut out by coring.**

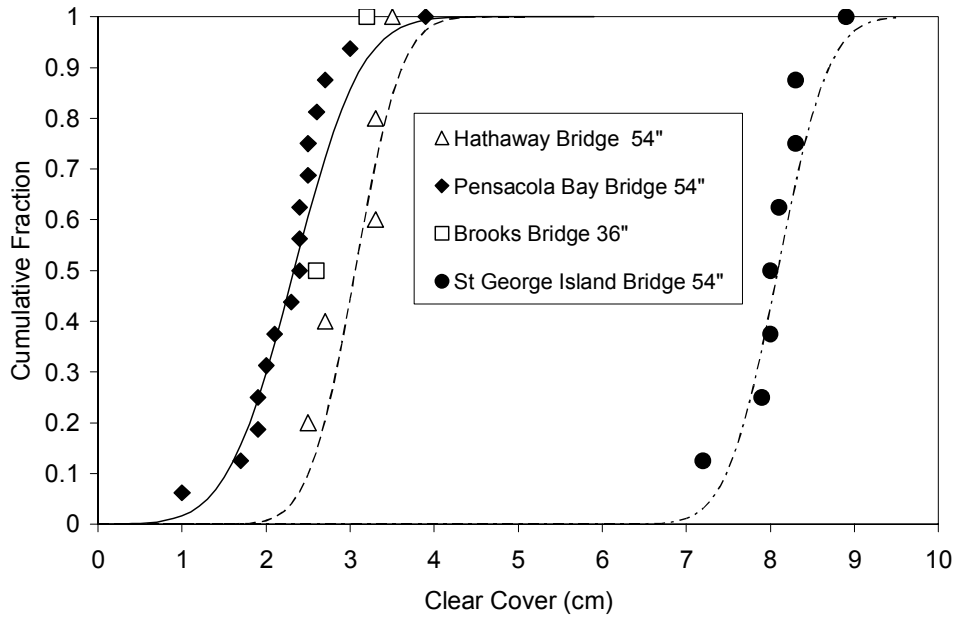


**FIGURE 4- Cumulative Fraction of Concrete Clear Cover to Spiral Wire.**

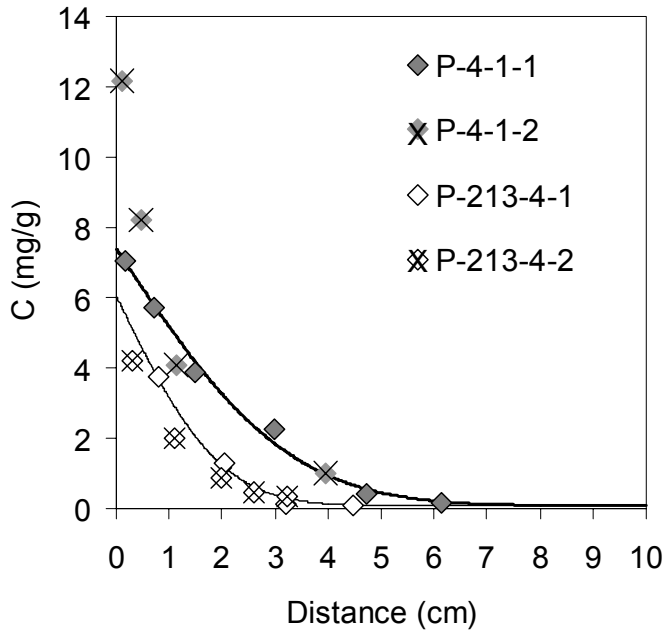


**FIGURE 5- Pensacola Bay Bridge Chloride Penetration Profiles. X, cracked companion core. Line, profiles per Eq. 1 for sound concrete.**

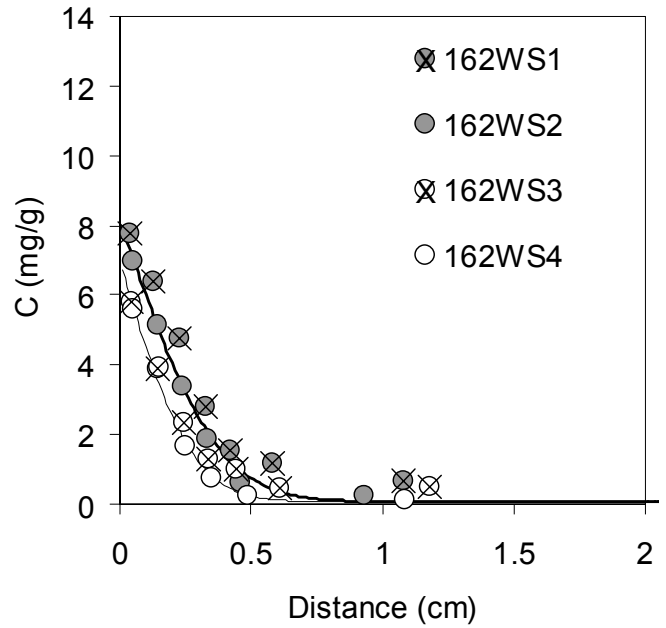


**FIGURE 6- St. George Island Bridge Chloride Penetration Profiles. X, cracked companion core. Line, profiles per Eq. 1 for sound concrete.**



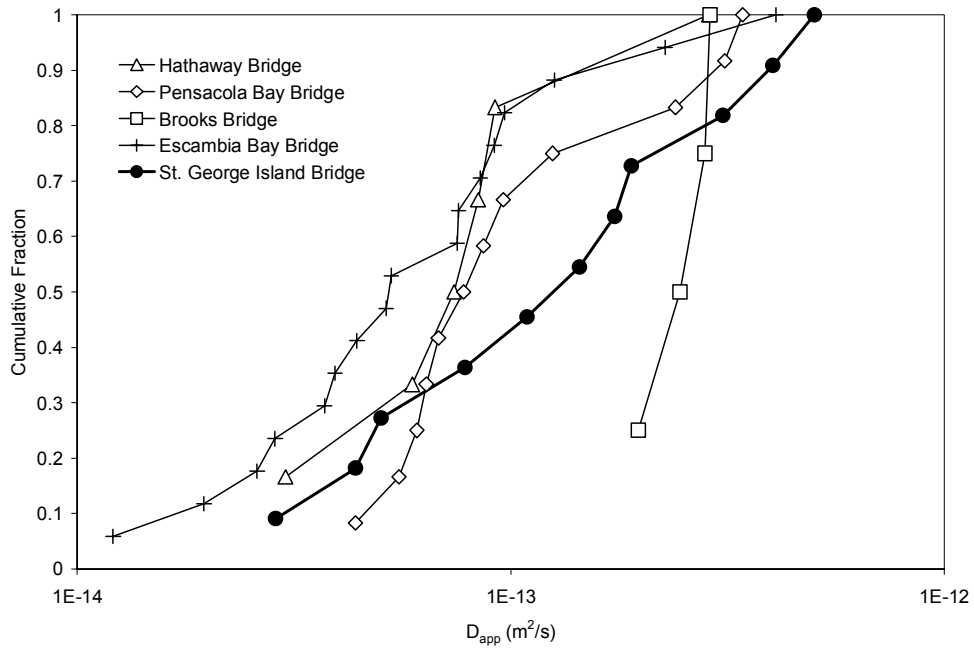


**FIGURE 7- Cumulative Fraction of  $D_{app}$  Values for Cylinder Piles in Present Investigation and Prior Escambia Bay Bridges Investigation.**

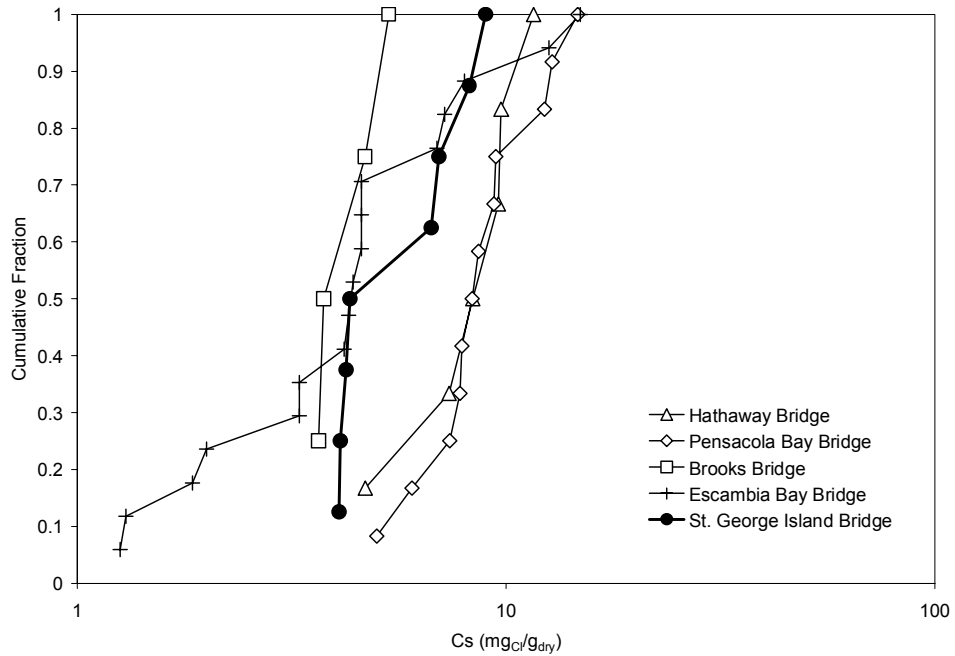


**FIGURE 8- Cumulative Fraction of  $Cs$  Values for Cylinder Piles in Present Investigation and Prior Escambia Bay Bridges Investigation.**

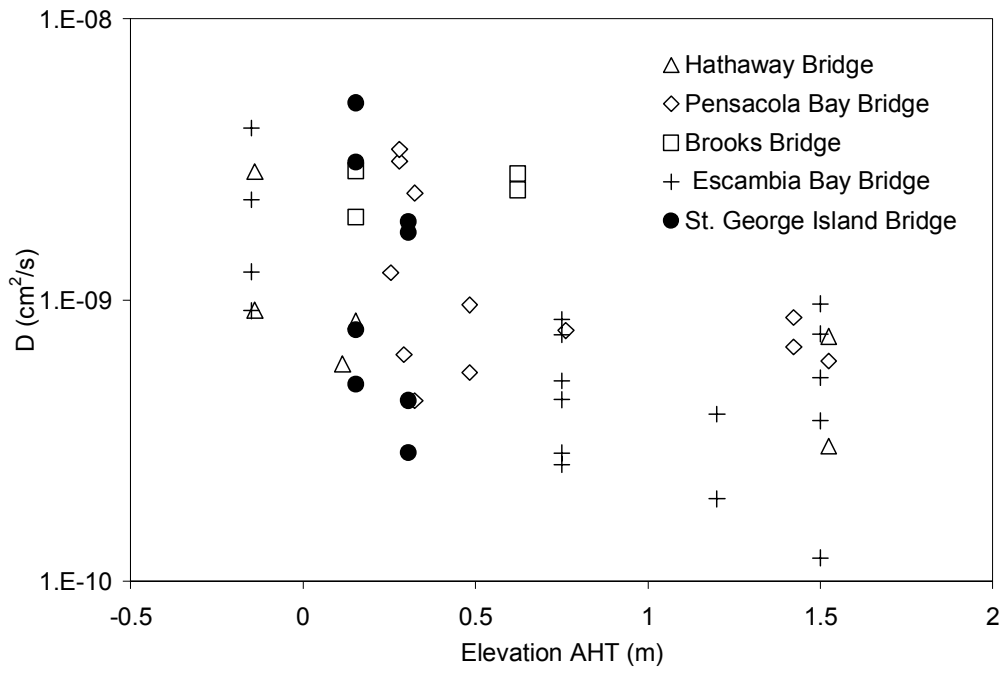


**FIGURE 9- Apparent Chloride Ion Diffusivity as Function of Core Elevation.**

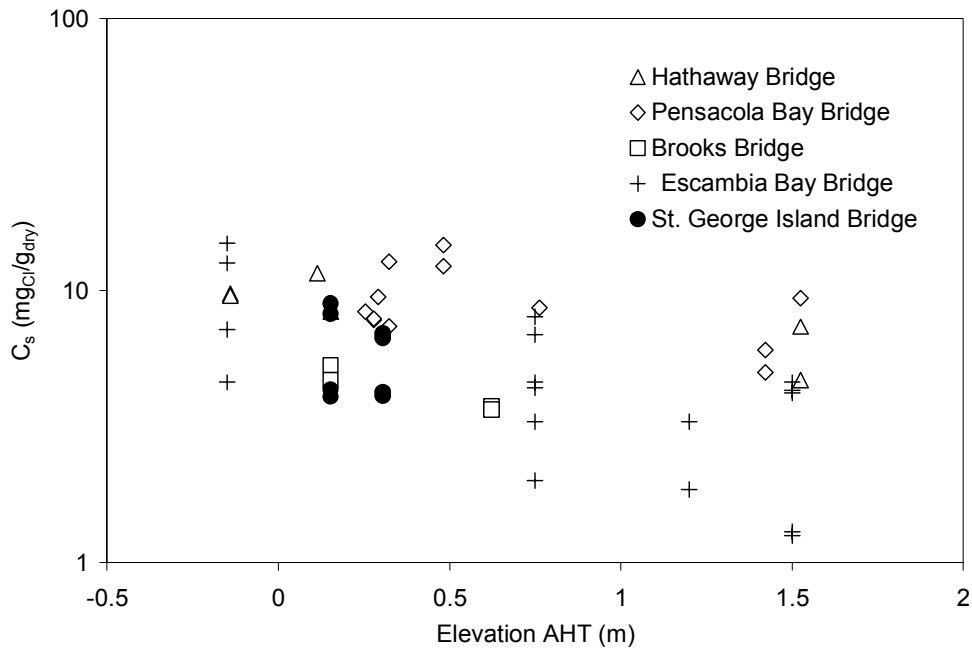


**FIGURE 10- Chloride Surface Concentration as Function of Core Elevation.**

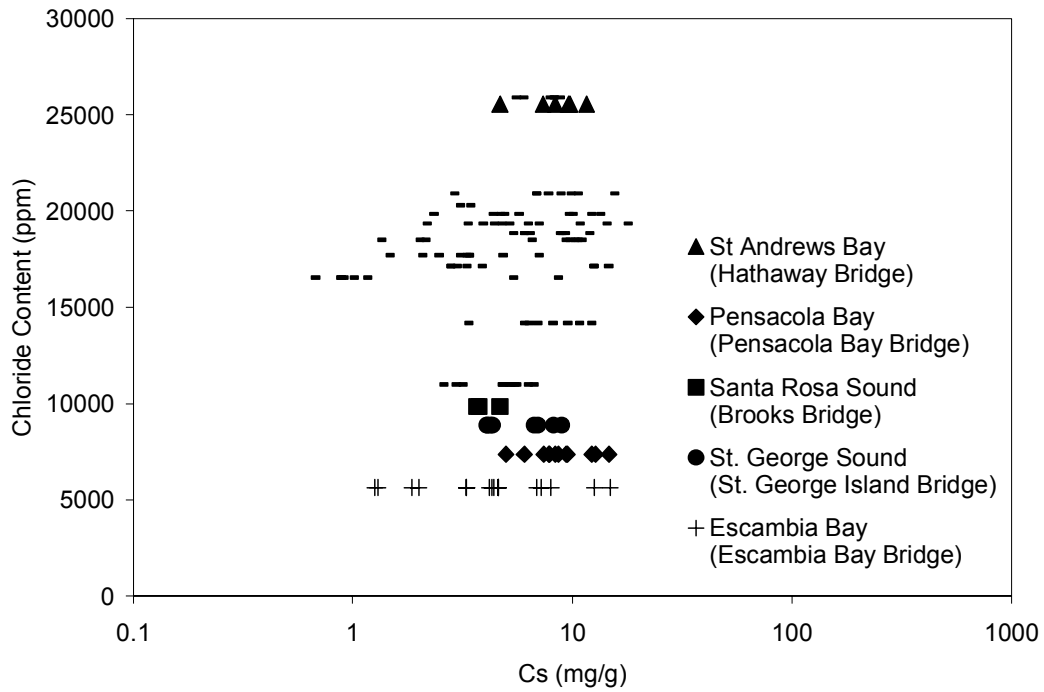


**FIGURE 11- Comparisons of Water Chloride Content and Concrete Chloride Surface Concentration  $C_s$  at Elevations -0.14 to 1.52 m AHT. Dash Symbols, Data for various bridges built with conventional modern concrete.**

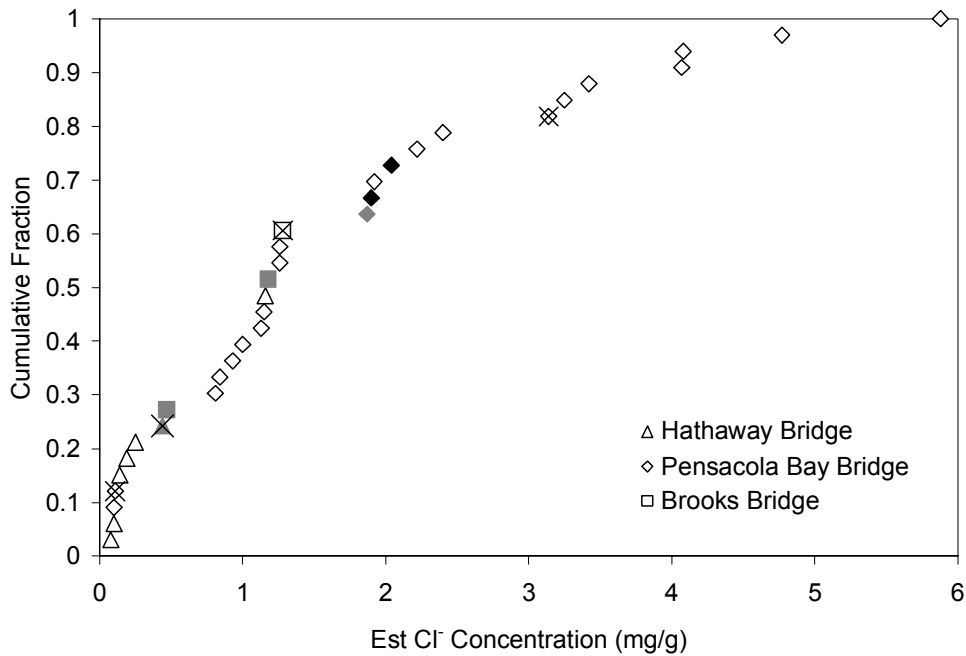


**FIGURE 12- Cumulative Fraction of Estimated Chloride Concentration at Steel Depth. Determined for locations where spiral or spacing bar steel was exposed by coring in the Hathaway, Pensacola, and Brooks bridges. Solid symbols, Severe corrosion. Grey symbols, Light corrosion. Open symbols, No corrosion. X, core drilled on crack.**

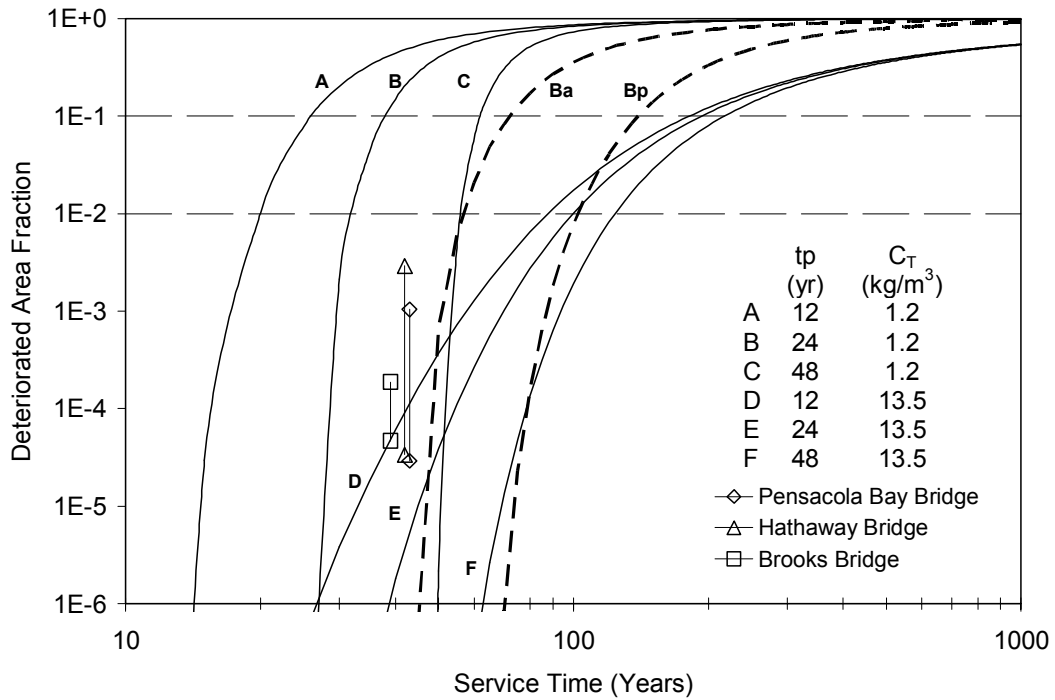


**FIGURE 13- Forecast deterioration model output. The vertical line represents the bounded range of observed damage at the time of the bridge survey. The horizontal dashed line corresponds to a 0.01 and 0.1 deterioration area fraction for nominal definitions of service life. The dashed model outputs represent the forecast deterioration of SGI Bridge piles with B input parameters for present X<sub>c</sub> (7.6 cm), B<sub>p</sub>, and for an alternative reduced X<sub>c</sub> (5.1 cm), B<sub>a</sub>.**